frontiers | Frontiers in Materials

TYPE Original Research
PUBLISHED 11 March 2025
DOI 10.3389/fmats.2025.1562267

OPEN ACCESS

EDITED BY
Mijia Yang,
North Dakota State University, United States

REVIEWED BY
Amir Ali Shahmansouri,
Washington State University, United States
Huixia Li,
Fujian University of Technology, China

*CORRESPONDENCE
Xiaolong Yang,
xiaolongyang@gxu.edu.cn

RECEIVED 17 January 2025
ACCEPTED 10 February 2025
PUBLISHED 11 March 2025

CITATION
Huang C, Zhu J, Rong H and Yang X (2025) Research on optimization design of high-performance manufactured sand concrete material composition in seasonal frozen areas.
Front. Mater. 12:1562267.
doi: 10.3389/fmats.2025.1562267

Research on optimization design of high-performance manufactured sand concrete material composition in seasonal frozen areas

Chuan Huang[1], Junxian Zhu[2], Hongliu Rong[2] and Xiaolong Yang[2]*

[1]Guangxi Zhuang Autonomous Region Road Development Center, Nanning, Guangxi, China, [2]School of Civil Engineering and Architecture, Guangxi University, Nanning, Guangxi, China

To address the issues of shrinkage cracking and durability in manufactured sand concrete in seasonally frozen regions, silica fume, fly ash, and superabsorbent polymer (SAP) were selected to prepare high-performance manufactured sand concrete. This study innovatively integrates SAP with fly ash and silica fume through a three-factor, four-level orthogonal experiment, systematically revealing their synergistic effects on workability, mechanical properties, and frost resistance—a gap in existing research. The results indicate that SAP improves the fluidity, workability, and slump of the concrete but reduces its mechanical properties. In contrast, silica fume and fly ash enhance the mechanical properties of the concrete. Notably, SAP's dual role in mitigating shrinkage (via internal curing) and frost damage (by pore structure optimization) is quantitatively established, with a 0.18% dosage reducing drying shrinkage by 13.4% and extending freeze-thaw resistance to 300 cycles. The optimized mix proportion for high-performance manufactured sand concrete is: water-to-cement ratio of 0.37, sand ratio of 42%, SAP content of 0.18%, silica fume content of 0.00%, and fly ash content of 15%. This study fills a research gap by quantitatively establishing the effects of SAP, fly ash, and silica fume on concrete performance in cold climates.

KEYWORDS

manufactured sand concrete, mechanical properties, SAP, mix proportion, workability

1 Introduction

With the depletion of natural river sand, manufactured sand concrete has been increasingly used in recent years for road concrete pavements and bridge deck overlays. However, due to the gradation or stone powder content of manufactured sand, the issue of shrinkage cracking in concrete pavements has become more severe (Cai et al., 2006; Yan et al., 2011; Bertelsen et al., 2020). The continuous appearance of cracks imposes a significant burden on the frost resistance and durability of concrete, accelerating freeze-thaw damage and performance degradation (Xu et al., 2004; Li, 2009; Ju et al., 2013), under the combined effects of traffic loads and other external forces, these issues can compromise the overall stability and durability of the road structure (Yuan et al., 2007; Ju et al., 2013). Therefore, it is imperative to develop an optimized mix proportion that can meet the

demands of complex climatic conditions and traffic loads while maintaining low production costs (Liu et al., 2013).

Significant progress has been made by researchers in the design and study of pavement concrete. Wang Shuotai (Wang et al., 2007), building upon classical mix design methods, specifically considered the influence of fly ash on concrete performance and independently developed a mix proportion suitable for high-performance pavement concrete. Experimental results showed that the flexural strength of concrete prepared using this method ranged from 6 to 10 MPa, demonstrating an improvement in the flexural strength of high-performance pavement concrete. Zhou et al. (2008) investigated the shrinkage properties of high-strength concrete made with natural sand and manufactured sand. The experimental results revealed that the shrinkage rate of manufactured sand high-strength concrete was higher than that of natural sand high-strength concrete during the first 7 days of curing. Moreover, manufactured sand concrete with a stone powder content of 7.0% exhibited superior drying shrinkage performance. Wang Jiliang (Ju et al., 2013) studied the factors influencing the salt-freezing resistance of pavement concrete, examining the effects of mineral admixtures, air-entraining agents, and water-cement ratios. The results indicated that a low water-cement ratio and high air content significantly improved the salt-freezing resistance of pavement concrete. Silica fume was found to markedly enhance salt-freezing resistance, with the optimal air content recommended to be above 3.8%. Furthermore, research (He and Lu, 2024) indicates that adding Expancel and air-entraining agents to cement mortar significantly improves its scaling resistance under freeze-thaw erosion. While the mechanical strength of the control group and samples with air-entraining agents decreased after freeze-thaw cycles, higher dosages of Expancel (1.5% and 2.0%) enhanced mechanical performance. Cao et al. (2007) conducted experiments on pavement concrete incorporating fly ash, silica fume, and air-entraining water reducers. By evaluating 13 mix proportions, it was found that pavement concrete with a 30% fly ash replacement rate, 7% silica fume content, and 1% air-entraining water reducer exhibited excellent frost resistance, low permeability, and relatively high flexural and compressive strength. Lao et al. (2021) introduced an internal curing material, SAP, into pavement concrete and analyzed its effects on shrinkage performance through concrete shrinkage deformation, internal humidity changes, microscopic morphology, and internal characteristics. The results showed that SAP promotes cement hydration, enhances the compactness of the internal structure, and reduces shrinkage deformation. Yu and Chen (2021) studied the mechanical properties, shrinkage behavior, and crack inhibition performance of high-adsorption stone powder manufactured sand concrete by incorporating expansive agents, shrinkage-reducing agents, polyvinyl alcohol fibers (PVA), and SAP. The experimental results revealed that all five methods effectively reduced early-age shrinkage cracking. Among them, PVA fibers and pre-saturated SAP significantly inhibited early-age shrinkage and cracking. Microstructural analysis further demonstrated that pre-saturated SAP promotes the hydration of cementitious materials, while PVA fibers improve the internal pore structure of concrete.

In summary, researchers globally have explored diverse strategies for enhancing concrete durability. For instance, recent studies by Snoeck et al. (2021b) demonstrated that SAP can act as both an internal curing agent and a crack-sealing material in cementitious systems under cyclic loading. Additionally, Mezhov (Hoque et al., 2025) highlighted the role of SAP in mitigating autogenous shrinkage in ultra-high-performance concrete (UHPC) through controlled water release.

Despite these advancements, two critical gaps remain: 1) Existing studies on SAP-modified concrete in seasonal frozen regions lack systematic optimization of multi-admixture synergies (e.g., SAP with fly ash/silica fume), particularly regarding workability-frost resistance trade-offs; 2) The interaction mechanisms between SAP-induced pore structures and freeze-thaw damage evolution are poorly understood at the microscale. This study employs SAP, silica fume, and fly ash as influencing factors to design an orthogonal experiment with three factors and four levels. The significance of these factors on the workability, mechanical properties, frost resistance, and shrinkage characteristics of high-performance manufactured sand concrete for pavements was analyzed. The primary evaluation indicators include 28-day flexural strength, 28-day drying shrinkage rate, and frost resistance grade, while secondary indicators consist of 7-day compressive strength, 7-day flexural strength, 28-day compressive strength, and slump. Comprehensive decision-making was conducted under specific climatic conditions to optimize the mix proportion of high-performance manufactured sand concrete for pavements.

Additionally, microstructural testing techniques, including scanning electron microscopy (SEM), were employed to analyze the microscopic morphology changes of concrete under the combined influence of SAP content and cyclic freeze-thaw conditions. By integrating the effect mechanisms of composite mineral admixtures on concrete, the study further elucidates the intrinsic relationship between the microstructure and macroscopic performance of high-performance manufactured sand concrete for pavements.

2 Materials and methodology

2.1 Raw materials

2.1.1 Cement

The cement used in this study is Qilianshan-brand ordinary Portland cement (PO 42.5). Its performance indicators were tested in accordance with the Testing Methods of Cement and Concrete for Highway Engineering (JTG 3420—2020) (Chinese Standards, 2021). Test results indicate an apparent density of 3.11 g/cm^3, with initial setting time reaching 225 min and final setting time attaining 301 min, all of which meet the specification requirements.

2.1.2 Fine aggregate

The fine aggregate used is basalt manufactured sand. Its technical specifications were tested according to the Construction sand (GB/T 14684-2022) (Chinese Standards, 2022), and the test results show that its bulk density is 2.795 g/cm^3, the fineness modulus is 2.9, the stone powder content is 2%, and the mica content is 0.1%, all of which meet the specifications. The gradation of the manufactured sand is presented in Table 1.

TABLE 1 Screening test results of machine-made sand.

Sieve size (mm)		4.75	2.36	1.18	0.6	0.3	0.15
Cumulative sieve residue (%)	Basalt	0.13	18.13	35.61	60.86	83.34	93.5
Technical requirements (%)	Upper limit	10	25	50	70	92	94
	Lower limit	0	0	10	41	70	80

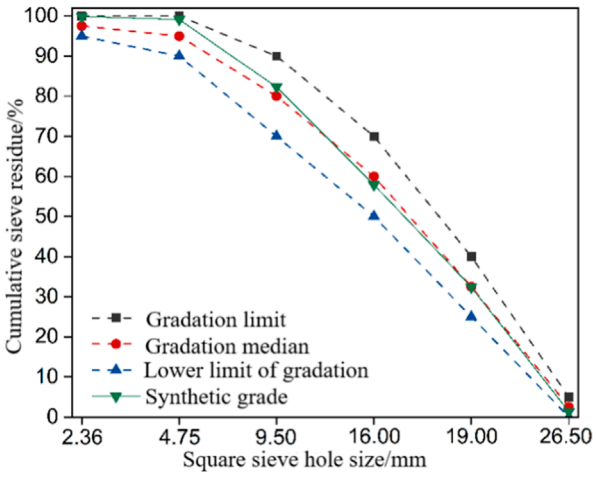

FIGURE 1
Coarse aggregate synthesis grading curve and specification range.

TABLE 2 SAP performance specifications.

Performance indicators	Unit	Specification requirement
Appearances	-	white granule
Particle size	μm	83–122
Absorption capacity	g/g	≥56
Centrifugal water retention	g/g	≥30
1-min pure water absorption	g/g	≥200
Salt water absorption rate	s	≤14
pH value	-	6.2
Residual monomer	PPM	<300

2.1.3 Coarse aggregate

The coarse aggregate used is basalt aggregate, with a particle size ranging from 5 to 26.5 mm. The test results show that its apparent density is 2.752 g/cm^3, which meets the experimental requirements. The gradation curve of the coarse aggregate is presented in Figure 1.

2.1.4 Water reducing agent

A high-performance polycarboxylate water-reducing agent is used, with a water-reducing rate ranging from 15% to 25%.

2.1.5 Fly ash and silica fume

The maximum incorporation rate of both silica fume and fly ash is selected as 9% (by mass). The fly ash used is Class F, Grade I. The test results show that its density is 2.0 g/cm^3 and its specific surface area is 445 m^2/kg, both of which meet the requirements. The bulk density of silica fume is 1,650 kg/m^3, with an average particle size of 1–5 μm and a specific surface area of 20–28 m^2/kg.

2.1.6 SAP

This study selected a polymer superabsorbent resin (SAP) with a mesh size of 100–120 mesh, and its specific performance specifications are shown in Table 2.

SAP exhibits a strong water absorption capacity, capable of absorbing hundreds of times its own weight in water, while also demonstrating excellent water retention properties to achieve long-term water storage. However, after releasing water molecules, SAP can create pore structures within the concrete, reducing the density of the concrete structure and thus lowering its mechanical strength. Furthermore, when the ion concentration and pH value of the pore solution inside the concrete increase, and the relative humidity decreases, SAP will release the stored water molecules, thereby promoting the hydration of the cement paste, while maintaining the internal environment of the concrete at a relatively high humidity to inhibit shrinkage. The water absorption capacity of SAP in concrete is influenced by the specific characteristics of the SAP itself. To measure SAP's absorption capacity, its water absorption in concrete is tested under simulated concrete conditions to determine its pre-absorbed water amount.

The method of introducing SAP directly affects the performance of the concrete. Simply incorporating SAP into the concrete without control over its absorption of water molecules from the cement paste will lead to excessive absorption of free water, resulting in a more viscous mix due to the lack of available free water. Conversely, insufficient water absorption will prevent SAP from exhibiting the desired absorption-release behavior. To mitigate the negative impact of direct SAP incorporation on concrete performance, pre-absorption with an appropriate absorption ratio is recommended.

Based on the mix proportion for high-performance concrete with manufactured sand for pavements, a cement paste solution was designed. The SAP's absorption-release characteristics were tested

TABLE 3 Water absorption test results of SAP pulp.

Group	SAP mesh size	SAP absorbed water (g)					Dry weight (g)	Wet weight (g)	Absorption ratio	Average absorption ratio
		0 min	5 min	10 min	30 min	1 h				
1	100–120	1.5	16.9	22.3	23.8	24.2	0.5	2	22.2	22.7
2		1.5	18.3	23.4	24.5	24.8			22.8	
3		1.5	18.7	24.1	24.9	25.1			23.1	

TABLE 4 Pavement mix design table of high-performance mechanical sand concrete.

W/C	Sand ratio	Water	Cement	Sand	Crushed stone	Water reducing agent (%)
0.37	0.42	155	420	786	1179	1.2%

using the tea bag method. The cement paste solution referenced the mix design from the pavement high-performance concrete with manufactured sand, as shown in Table 10. The SAP absorption-release tests were conducted by weighing 1 g of SAP in three separate trials, along with the dry weight of nylon tea bags. The SAP was then placed in the tea bags and immersed in the prepared cement paste, where the weight of the SAP was measured at different time intervals until the absorption-release characteristics reached equilibrium.

The results of the SAP absorption-release measurements in the cement paste are shown in Table 3.

As shown in Table 3, the test evaluated the SAP absorption within 1 h. Three parallel tests were performed to reduce experimental errors, and the arithmetic mean was taken as the final value. In the cement paste solution, the SAP absorption ratio increased with time. The absorption rate was highest during the first 5 min, showing a linear increase, and then slowed down after 10 min, stabilizing around 30 min. By 1 h, the absorption rate nearly plateaued. Therefore, SAP's absorption behavior in concrete mainly occurs during the first 10 min, with an absorption ratio of around 25 times. Based on these findings, it is recommended that the pre-absorbed water ratio of SAP be set at 25 times when incorporated as an admixture in concrete.

2.2 Methodology

2.2.1 Concrete mix design

According to the Technical Guidelines for Construction of Highway Cement Concrete Pavements requirements (Chinese Standards, 2019b) and Technical specification for application of high-performance concrete (Chinese Standards, 2006), which outline the requirements for pavement concrete's flexural strength (≥5.0 MPa) and durability under freeze-thaw conditions, the water-cement ratio for high-performance concrete is determined to be 0.37, with a cement content of 420 kg/m^3. The sand ratio of 42% was optimized through preliminary trials to balance workability and mechanical performance, considering the angular particle morphology of basalt manufactured sand. The specific concrete mix design is shown in Table 4.

2.2.2 Factors and level combinations

The dosages of SAP, silica fume, and fly ash were selected as the factors for this study. SAP dosage levels (0%–0.18%) were selected based on preliminary rheology tests indicating severe slump loss (>40%) at >0.2% SAP due to excessive water absorption. This range aligns with Snoeck et al. (2017) recommendations for SAP in arid climates, where lower dosages prevent over-porosity while maintaining internal curing efficacy. The levels of these factors are shown in Table 5. The experimental design was based on the L16 (4^3) orthogonal test, with the factor levels and combinations given in Table 6.

2.2.3 Orthogonal test evaluation indicators and experimental methods

To obtain a high-performance mechanical sand concrete mix suitable for seasonal freeze-thaw regions, the primary evaluation indicators selected were 28-day flexural strength, 28-day compressive strength, 28-day drying shrinkage rate, 28-day frost resistance grade, and slump. The secondary evaluation indicators were 7-day flexural strength and 7-day compressive strength. The study aims to investigate the significance of each factor and determine the optimal level combination of the pavement high-performance mechanical sand concrete under different influences.

For specific testing, the slump test of the concrete was conducted according to the relevant standards in the Standard for test method of performance on ordinary fresh concrete (GB/T 50080-2016) (Chinese Standards, 2017). Flexural and compressive strengths were tested according to the Standard for test methods of concrete physical and mechanical properties (GB/T 50081-2019) (Chinese Standards, 2019a). The frost resistance and shrinkage properties of the concrete were tested according to the Standard test method for long term performance and durability of ordinary concrete (GB/T 50082-2009) (Chinese Standards, 2010).

2.2.4 SEM analysis

To further investigate the effect of SAP content on the frost resistance of concrete under freeze-thaw conditions, concrete specimens with SAP content of 0.00% were selected for 0, 150 freeze-thaw cycles, and specimens with SAP content of 0.18% were selected for 0, 150, and 250 freeze-thaw cycles. SEM was employed to observe

10.3389/fmats.2025.1562267

TABLE 5 Horizontal table of orthogonal test factors.

Factor level	SAP dosage (A) %	Silica fume dosage (B) %	Fly ash dosage (C) %
1	0.12	9	0
2	0.06	6	3
3	0	3	9
4	0.18	0	6

TABLE 6 Orthogonal test table of high-performance mechanical sand concrete L16 (4^3) for pavement.

Test number	Factor classification				Level combination
	A	B	-	C	
L1	1	1	1	1	$A_1B_1C_1$
L2	1	2	2	2	$A_1B_2C_2$
L3	1	3	3	3	$A_1B_3C_3$
L4	1	4	4	4	$A_1B_4C_4$
L5	2	1	2	3	$A_2B_1C_3$
L6	2	2	1	4	$A_2B_2C_4$
L7	2	3	4	1	$A_2B_3C_1$
L8	2	4	3	2	$A_2B_4C_2$
L9	3	1	3	4	$A_3B_1C_4$
L10	3	2	4	3	$A_3B_2C_3$
L11	3	3	1	2	$A_3B_3C_2$
L12	3	4	2	1	$A_3B_4C_1$
L13	4	1	4	2	$A_4B_1C_2$
L14	4	2	3	1	$A_4B_2C_1$
L15	4	3	2	4	$A_4B_3C_4$
L16	4	4	1	3	$A_4B_4C_3$

the changes in the microstructure of the concrete, focusing on the micro morphology and the interfacial transition zone (ITZ).

3 Results and discussion

3.1 Workability

The slump test results of different types of mechanical sand concrete are shown in Figure 2.

As shown in Figure 2, the slump values for L5–L11 are relatively low, ranging from 20 mm to 35 mm, while the slump values for L1–L4 and L12–L16 are higher, ranging from 40 mm to 65 mm. The primary reason for this difference is the varying amounts of admixtures and mineral admixtures, which result in different slump values for the fresh concrete. The SAP, after absorbing water, increases the flowability, workability, and slump of the fresh concrete, with the slump increasing as the SAP content rises (Chitthawornmanee et al., 2025). The reason lies in the fact that SAP absorbs part of the free water during the early mixing stage, temporarily reducing the flowability of the system. However, over time (such as during cement hydration or material hardening), SAP gradually releases water, replenishing the moisture lost due to evaporation or reaction, thereby extending the system's "open

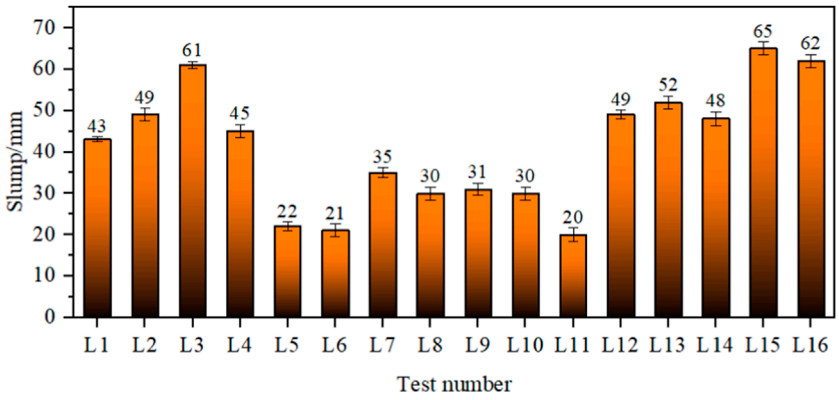

FIGURE 2
Slump of pavement high-performance mechanical sand concrete.

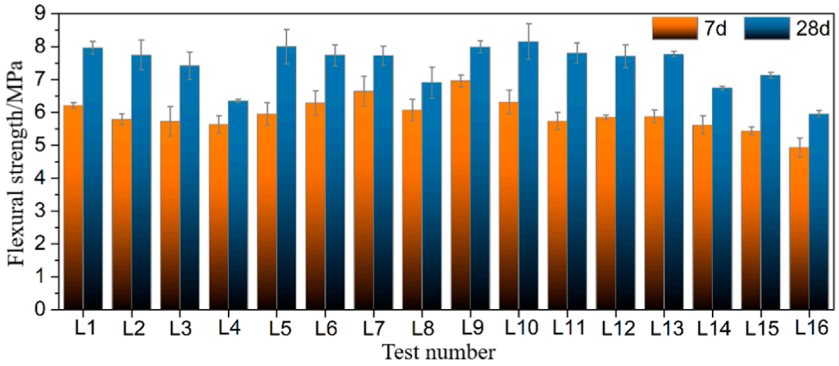

FIGURE 3
7-day and 28-day flexural strength.

time" (workability window). This process is similar to internal curing, where the moisture distribution is dynamically regulated to prevent premature drying or hardening (Hansen, 2001). The characteristics of mineral admixtures, particularly silica fume, such as its light weight, large specific surface area, small particle size, and high water absorption, play a significant role in concrete behavior. The addition of silica fume increases the viscosity of the paste through mechanisms such as the filling effect and secondary hydration reactions. This increase in viscosity makes the concrete more viscous during mixing and pouring, which in turn affects its flowability, slump, and workability. Moreover, higher silica fume content leads to an increased water demand, further decreasing the flowability, slump, and workability of fresh concrete (Li et al., 2024; Zhang et al., 2024).

3.2 Mechanical property

The test results of different level combinations of mechanical sand concrete, evaluated based on 7-day and 28-day flexural strength, are shown in Figure 3.

In L12, the dosages of SAP, silica fume, and fly ash are all 0.00%, making it the control group for comparison. From Figure 3, it can be observed that the flexural strength of the pavement high-performance machine-made sand concrete specimens increases with age. In the control group L12, the 7-day and 28-day flexural strengths are 5.85 MPa and 7.71 MPa, respectively. Statistical analysis of the flexural strength of the 16 test groups shows that the average 7-day flexural strength is 5.91 MPa, and the average 28-day flexural strength is 7.46 MPa, indicating an increase of 26.23% as the age increases from 7 to 28 days. Compared to L12, the average 7-day flexural strength of the concrete is similar to that of L12, while the average 28-day flexural strength is 0.25 MPa lower than L12, a reduction of 3.24%. At 7 days, L9 has the highest flexural strength, with a value of 6.96 MPa, while L16 has the lowest flexural strength, with a value of 4.93 MPa, showing a difference of 29.2%. At 28 days, L10 has the highest flexural strength, with a value of 8.35 MPa, while L16 has the lowest flexural strength, with a value of 5.95 MPa, showing a difference of 28.7%. The 7-day and 28-day flexural strengths of L4 are 5.63 MPa and 6.35 MPa, respectively, indicating that the influence of age on concrete strength is minimal for this combination.

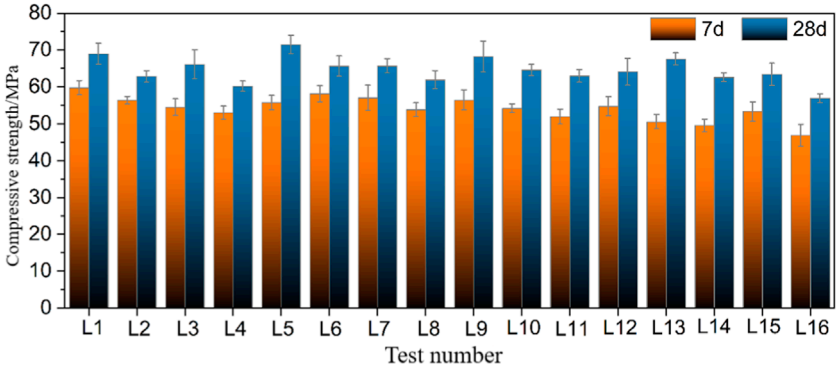

FIGURE 4
7-day and 28-day compressive strength.

The 7-day and 28-day compressive strength results of the different level combinations of the machine-made sand concrete are shown in Figure 4.

As shown in Figure 4, the compressive strength of high-performance machine-made sand concrete increases with age. In the baseline group L12, the 7-day and 28-day compressive strengths are 54.78 MPa and 64.13 MPa, respectively. Statistical analysis of the 16 test groups shows that the average 7-day compressive strength is 54.17 MPa, and the average 28-day compressive strength is 64.60 MPa, with an increase of 19.25% from 7 days to 28 days. Compared to L12, the 7-day and 28-day compressive strengths of the concrete are not significantly different. At 7 days, L1 has the highest compressive strength at 59.78 MPa, while L16 has the lowest at 46.96 MPa. At 28 days, L5 has the highest compressive strength at 71.51 MPa, and L16 has the lowest at 56.94 MPa. Among L1–L16, only L14 and L16 have a 7-day compressive strength below 50.0 MPa, and L16 has a 28-day compressive strength below 60.0 MPa; the rest are all above 60.0 MPa.

These results suggest that the incorporation of SAP reduces the mechanical properties of machine-made sand concrete, while the inclusion of mineral admixtures, particularly silica fume, enhances its mechanical performance.

3.3 28-day drying shrinkage rate

Considering the adverse impact of seasonal freezing-thawing zones on the shrinkage properties of high-performance concrete, the absorption-desorption characteristics of SAP were utilized to reduce the shrinkage performance of concrete. The test results of the 28-day drying shrinkage rate for different specimens are shown in Figure 5.

As shown in Figure 5, the 28-day drying shrinkage rate varies significantly among different combinations. The reference group, L12, has a 28-day drying shrinkage rate of 505×10^{-6}, while the maximum drying shrinkage rate is observed in L9, at 620.4×10^{-6}, and the minimum shrinkage rate is found in L2, at 450×10^{-6}. Compared to L12, groups with SAP contents of 0.06%, 0.12%, and 0.18% show lower shrinkage rates, indicating that the inclusion of SAP reduces the drying shrinkage of concrete. This is because SAP releases its stored water molecules, promotes the hydration of the paste, and maintains the internal environment of the concrete at a relatively high humidity, thus inhibiting shrinkage. When comparing L13, L15, and L16, it is observed that with an increase in fly ash content, the drying shrinkage rate of the concrete initially decreases and then increases. This suggests that fly ash improves the shrinkage performance of concrete, but excessive amounts of fly ash reduce the shrinkage performance. The main reasons are that fly ash improves shrinkage resistance through the following mechanisms: 1) the delayed pozzolanic reaction reduces early thermal stress, but fly ash undergoes a pozzolanic reaction with calcium hydroxide, this reaction is generally slower than the hydration of cement. Excessive fly ash can delay the formation of the hydration products, such as calcium silicate hydrate (C-S-H), which are responsible for reducing shrinkage. 2) the spherical particles enhance the packing density of the particles. Comparing L12 and L14, L14 has a higher shrinkage rate than L12, even though the SAP content is 0.18% and the micro-silica content is 6%. This indicates that an increase in silica fume content also increases the drying shrinkage of concrete.

3.4 Frost durability

The freeze-thaw cycle test was conducted on different concretes, and the relative dynamic modulus of elasticity of the concrete is shown in Figure 6. The freeze-thaw resistance grade of the concrete is shown in Figure 7.

As shown in Figure 6A, the relative dynamic modulus of elasticity (P) for L1–L4 decreases with the increase in freeze-thaw cycles. Specifically, L1–L2 show a sharp decrease after 75 cycles, while L3 decreases sharply after 100 cycles. At 125 cycles of freeze-thaw, the P value for L1 is 82.7%, and when the cycles reach 150, cracks appear on the surface of the concrete, indicating that L1 concrete specimens have been damaged. For L2, at 100 cycles, P2 is 79.6%, and cracks appear at 125 cycles, signifying damage to the L2 specimen. For L3, at 150 cycles, P3 is 79.8%, and after this point, cracking and damage begin. At 300 freeze-thaw cycles, P4 for L4 is 70.4%, indicating that the freeze-thaw resistance grade F of L4 reaches 300 cycles. The variation in freeze-thaw resistance cycles among different concrete specimens is mainly due to the different silica fume contents, which shows that silica fume decreases

10.3389/fmats.2025.1562267

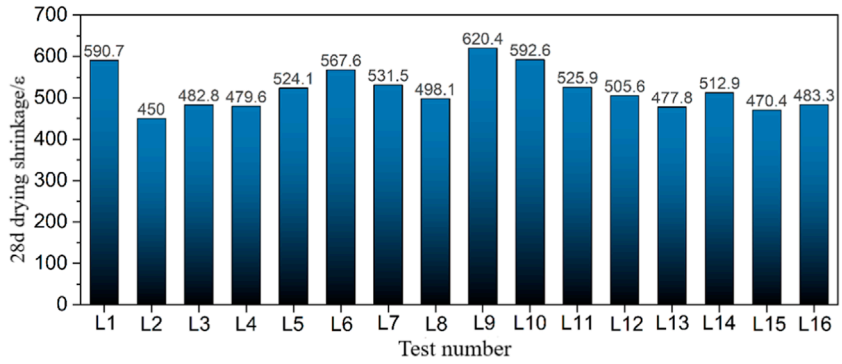

FIGURE 5
28-day drying shrinkage rate of concrete specimens.

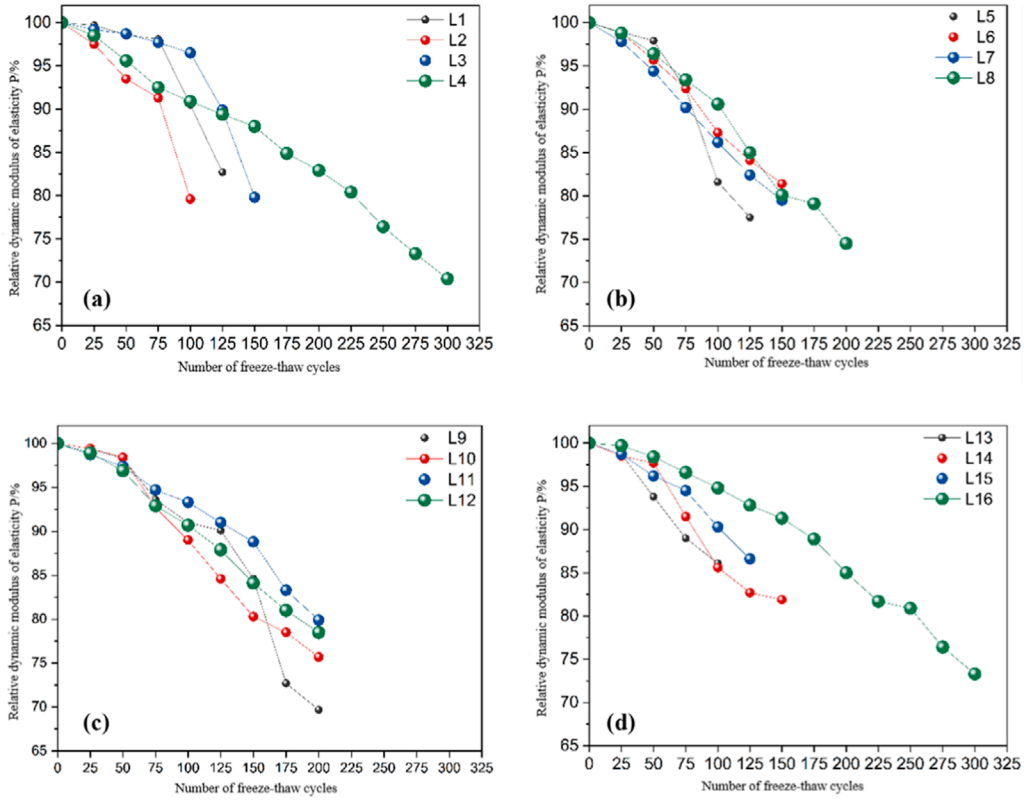

FIGURE 6
Relative dynamic modulus of elasticity of concrete. **(A)** L1-L4. **(B)** L5-L8. **(C)** L9-L12. **(D)** L13-L16.

the freeze-thaw resistance of concrete. Silica fume's adverse impact on frost resistance stems from over-densification: While its nano-filler effect reduces macropores (>100 nm), it increases microcrack susceptibility under freeze-thaw cycles due to brittleness. This aligns with Zhang et al. (2021) findings that silica fume content >6% compromises concrete's strain capacity.

As shown in Figures 6B, C, the relative dynamic modulus of elasticity for L5–L8 decreases with the increase in freeze-thaw cycles. When these specimens fail, the relative dynamic modulus of elasticity for the concrete is 77.5%, 81.4%, 79.5%, and 74.5%, respectively. The freeze-thaw resistance grades are 125, 150, 150, and 200 cycles, respectively. For L9–L12, the specimens fail after more than 200 freeze-thaw cycles, and the relative dynamic modulus of elasticity decreases with the increase in freeze-thaw cycles. At the point of failure for L9–L12, the relative dynamic modulus of elasticity for the concrete is 69.7%, 75.7%, 79.9%, and 78.5%, respectively. The loss rates of dynamic modulus of elasticity are 30.3%, 24.3%, 20.1%, and 21.5%, respectively.

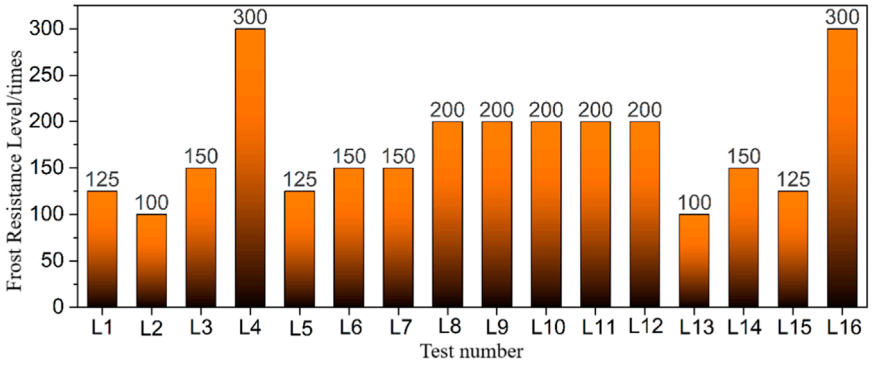

FIGURE 7
Freeze-thaw resistance grade of concrete for pavements.

As shown in Figure 6D, L13 (with SAP content of 0.18%, silica fume content of 9.0%, and fly ash content of 3.0%) exhibits the worst freeze-thaw resistance. After 100 freeze-thaw cycles, its relative dynamic modulus of elasticity (P13) is 86.1%, with a dynamic modulus loss rate of 13.9%. This indicates that the mechanical properties and rigidity of the concrete specimen are significantly affected when failure occurs, suggesting a combination of freeze-thaw damage and mechanical failure.

For L14, after 175 freeze-thaw cycles, cracks appear on the surface of the concrete specimen, indicating that it has failed. After 150 freeze-thaw cycles, P14 is 81.9%, with a dynamic modulus loss rate of 18.1%, and its freeze-thaw resistance grade (F) is 150 cycles. Compared to L13, the freeze-thaw resistance grade increases from 100 cycles to 150 cycles when the silica fume content decreases from 9.0% to 6.0%, representing a 30.0% improvement in freeze-thaw performance. Therefore, the silica fume content is inversely proportional to the concrete's freeze-thaw performance.

L15 fails after 150 freeze-thaw cycles, with a freeze-thaw resistance grade of 125 cycles. The relative dynamic modulus is 86.6%, and the dynamic modulus loss rate is 13.4%. L16, however, shows a freeze-thaw resistance grade of 300 cycles. After 300 freeze-thaw cycles, the relative dynamic modulus of elasticity is 73.3%, with a loss rate of 26.7%.

Based on Figures 6, 7, the deterioration pattern of the freeze-thaw resistance of high-performance mechanical sand concrete can be summarized as follows: The reduced frost resistance with silica fume is attributed to its nano-filler effect, which densifies the matrix but increases brittleness. This brittleness promotes microcrack propagation under freeze-thaw cycles; Fly ash improves frost resistance by refining pore structure through pozzolanic reactions, reducing harmful pores (>50 nm). SAP enhances frost resistance via two mechanisms: 1) water release buffers ice crystallization pressure (Snoeck et al., 2021a), and 2) its spherical pores act as stress-relief chambers, reducing internal cracking; when the number of freeze-thaw cycles is less than or equal to 50, the decline in freeze-thaw resistance is slow. Between 50 and 150 cycles, the deterioration rate increases significantly. After 150 cycles, the decline in freeze-thaw resistance slows down gradually until freeze-thaw failure occurs.

3.5 Impact of fly ash and silica fume on concrete

The use of fly ash and silica fume in concrete has a significant impact on the workability, compressive strength, and freeze-thaw durability of concrete in seasonal freeze-thaw regions. Fly ash, as a mineral admixture, improves the workability of concrete, particularly in enhancing its flowability. The fine particles of fly ash can fill the voids between cement particles, reducing friction and improving the flowability of the mix. Additionally, fly ash helps lower the heat of hydration of the cement, which can prevent early cracking in cold environments.

Silica fume, on the other hand, primarily enhances concrete properties through its high reactivity, which promotes the formation of additional C-S-H gel during cement hydration. This further improves the flowability and cohesiveness of the concrete mix. When used in combination with fly ash, silica fume compensates for the early strength loss caused by fly ash, ensuring that the concrete performs well in freeze-thaw conditions typical of seasonal freeze-thaw regions.

In terms of compressive strength, fly ash improves the long-term strength of concrete but may reduce early strength. Silica fume, however, significantly enhances early strength, which helps offset the early strength loss associated with fly ash. The combined use of fly ash and silica fume achieves a balance between early and long-term strength, making it suitable for concrete in seasonal freeze-thaw regions.

Regarding freeze-thaw durability, fly ash reduces the porosity and improves the density of the concrete, thereby decreasing water absorption and enhancing freeze-thaw resistance. Silica fume further refines the microstructure, increasing the density of the concrete and reducing the formation of microcracks during freeze-thaw cycles. Therefore, the synergistic effect of fly ash and silica fume significantly improves the freeze-thaw durability of concrete, minimizing the damage caused by freeze-thaw cycles.

In conclusion, the combined use of fly ash and silica fume effectively enhances the workability, compressive strength, and freeze-thaw durability of concrete. Their synergistic effects result in concrete that performs well under freeze-thaw conditions, making it suitable for construction in cold climates.

3.6 Microstructural changes

The microstructural morphology of high-performance mechanical sand concrete under the interaction of SAP content and freeze-thaw cycles is shown in Figures 8A–J.

As shown in Figure 8, the hydration products in the concrete microstructure decrease with the increase in freeze-thaw cycles, and the compactness of the microstructure gradually loosens. At 150 freeze-thaw cycles, the concrete with 0.18% SAP content shows a higher degree of microstructural compaction. Figures 8A, B show that the microstructure of SAP 0.00%-0F contains abundant cementitious material hydration products, such as flocculent C-S-H, and the ITZ between aggregates and cement paste is clearly visible.

Figures 8C, D demonstrate the microstructure of SAP 0.00%-150F concrete. In addition to the large amount of flocculent C-S-H, the freeze-thaw cycles at 150 times cause the cement-based materials to become more porous. Figures 8E, F show that the hydration products of SAP 0.18%-0F contain a large amount of flocculent C-S-H, needle-like AFt, and layered CH. Compared to SAP 0.00%-0F, the hydration products are richer in both content and type, indicating that the incorporation of SAP promotes the hydration of cementitious materials. Figure 8H displays the ITZ in SAP 0.18%-150F concrete. After 150 freeze-thaw cycles, the ITZ remains intact with no signs of deterioration.

As shown in Figure 8I, the SAP 0.18%-250F microstructure contains a large amount of C-S-H, AFt, and pore structures, and the ITZ remains intact even after 250 freeze-thaw cycles, without any signs of deterioration. This can be attributed to the spherical shape of SAP after water absorption, which, when incorporated into concrete, increases the porosity of the concrete. As water molecules in the capillary pore structure expand due to crystallization effects and phase transformation, the increased volume can be stored in certain areas. This reduces the expansion pressure on the capillary pore walls while promoting the migration and redistribution of crystalline water molecules in the micro-pore structure, thereby reducing the concrete's osmotic pressure. This phenomenon further proves that SAP enhances the freeze-thaw durability of concrete.

The enhancement of freeze-thaw resistance by SAP can be attributed to their dual role in pore structure modification and internal curing. SAPs absorb excess mixing water, forming macro-pores upon drying, which act as expansion reservoirs to accommodate ice formation, thereby reducing internal stress during freezing (Mechtcherine et al., 2015). Concurrently, the gradual release of absorbed water during hydration promotes continued cement hydration, refining the capillary pore structure and lowering the overall water saturation degree—a critical factor in freeze-thaw durability (Craeye et al., 2011). Experimental studies using mercury intrusion porosimetry (MIP) have shown that SAP-modified concrete exhibits a more homogeneous pore distribution with reduced harmful micropores (<50 nm), decreasing the likelihood of critical ice crystallization (Liu et al., 2019).

In conclusion, SAPs improve freeze-thaw resistance by redistributing water, refining pore structure, inhibiting ice growth, and dissipating stresses, supported by A lot of experimental evidence. Their multifunctional role positions SAPs as a promising additive for durable concrete in cold climates.

3.7 Analysis of the relationship between single factors and multiple evaluation indicators

The variation in slump of high-performance manufactured sand concrete for pavements with different dosages of SAP, silica fume, and fly ash is shown in Figure 9.

As shown in Figure 9A, the slump of high-performance manufactured sand concrete initially decreases and then increases with the increase in SAP content. When the SAP content increases from 0.00% to 0.18%, the slump increases from 32.5 mm to 56.75 mm, representing a 74.6% increase. The increase in silica fume content has little significant effect on the slump; as the content increases from 0.00% to 9.00%, the slump gradually decreases from 46.5 mm to 37 mm. The variation in fly ash content also has a minimal impact on slump, with the slump fluctuating by only about 6 mm within the range of 0.00%–9.00%. In conclusion, SAP has a significant effect on slump, with an optimal content of 0.18%, while the effects of silica fume and fly ash are relatively limited.

As shown in Figure 9B, the early compressive strength of high-performance manufactured sand concrete first increases and then decreases with the increase of SAP content. It increases with the increase of silica fume content, while the effect of fly ash content on the early compressive strength of concrete is not significant. The factor that has the greatest impact on the early compressive strength of concrete is SAP. When the SAP content increases from 0.00% to 0.12%, the compressive strength increases by 2.83%. However, when the content reaches 0.18%, the compressive strength is the lowest, indicating that the inclusion of SAP reduces the early compressive strength of concrete.

As shown in Figure 9C, the 7-day flexural strength of concrete with manufactured sand initially increases and then decreases as the SAP content increases. A slight increase is observed when the SAP content is 0.06%, but at 0.18% SAP, the flexural strength decreases by 10.93%. The flexural strength increases with the increase in micro-silica content, with the maximum increase being 11.21%. The strength decreases with the increase in fly ash content, with a reduction of 7.23% when the fly ash content reaches 9%. Therefore, the incorporation of silica fume enhances the 7-day flexural strength of concrete, while the addition of SAP and fly ash decreases it.

As shown in Figure 9D, the 28-day compressive strength of concrete first increases and then decreases with the increase in SAP content, increases with the addition of silica fume, and first decreases and then increases with the addition of fly ash. The maximum decrease in compressive strength due to the incorporation of SAP was 3.23%. When the SAP content increased from 0.0% to 0.06%, the 28-day compressive strength of concrete showed a slight increase. This may be because the appropriate amount of SAP improved the workability of the concrete, allowing the cementitious materials to better bond together, which increased the density of the concrete material. The addition of silica fume resulted in a maximum increase

10.3389/fmats.2025.1562267

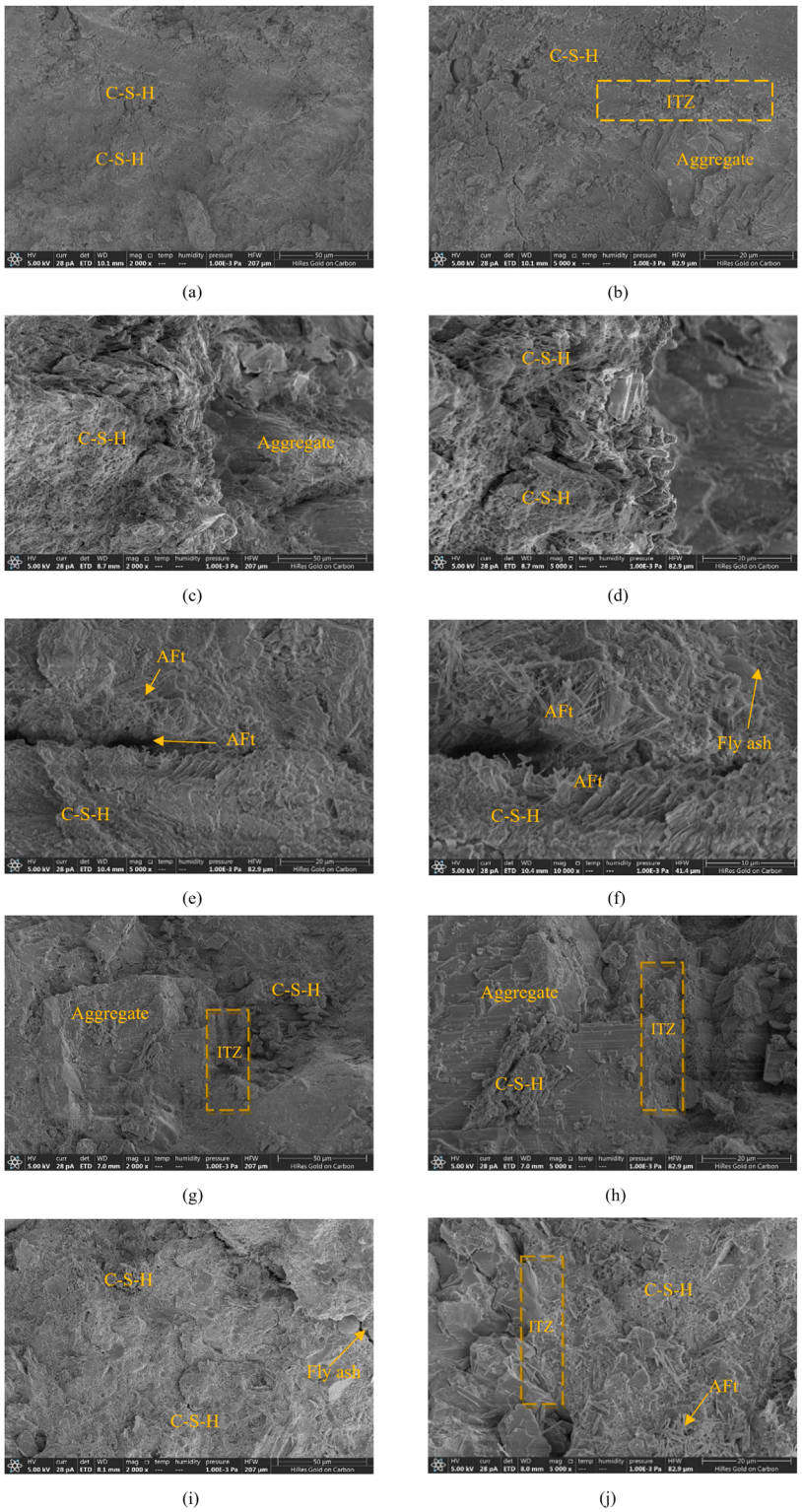

FIGURE 8
Microstructural morphology of concrete under freeze-thaw cycles and SAP content. **(A)** SAP0.00%-0F (×5000). **(B)** SAP0.00%-0F (×10000). **(C)** SAP0.00%-150F (×5000). **(D)** SAP0.00%-150F (×10000). **(E)** SAP0.18%-0F (×5000). **(F)** SAP0.18%-0F (×10000). **(G)** SAP0.18%-150F (×5000). SAP0. **(H)** 18%-150F (×10000). **(I)** SAP0.18%-250F (×5000). **(J)** SAP0.18%-250F (×10000).

10.3389/fmats.2025.1562267

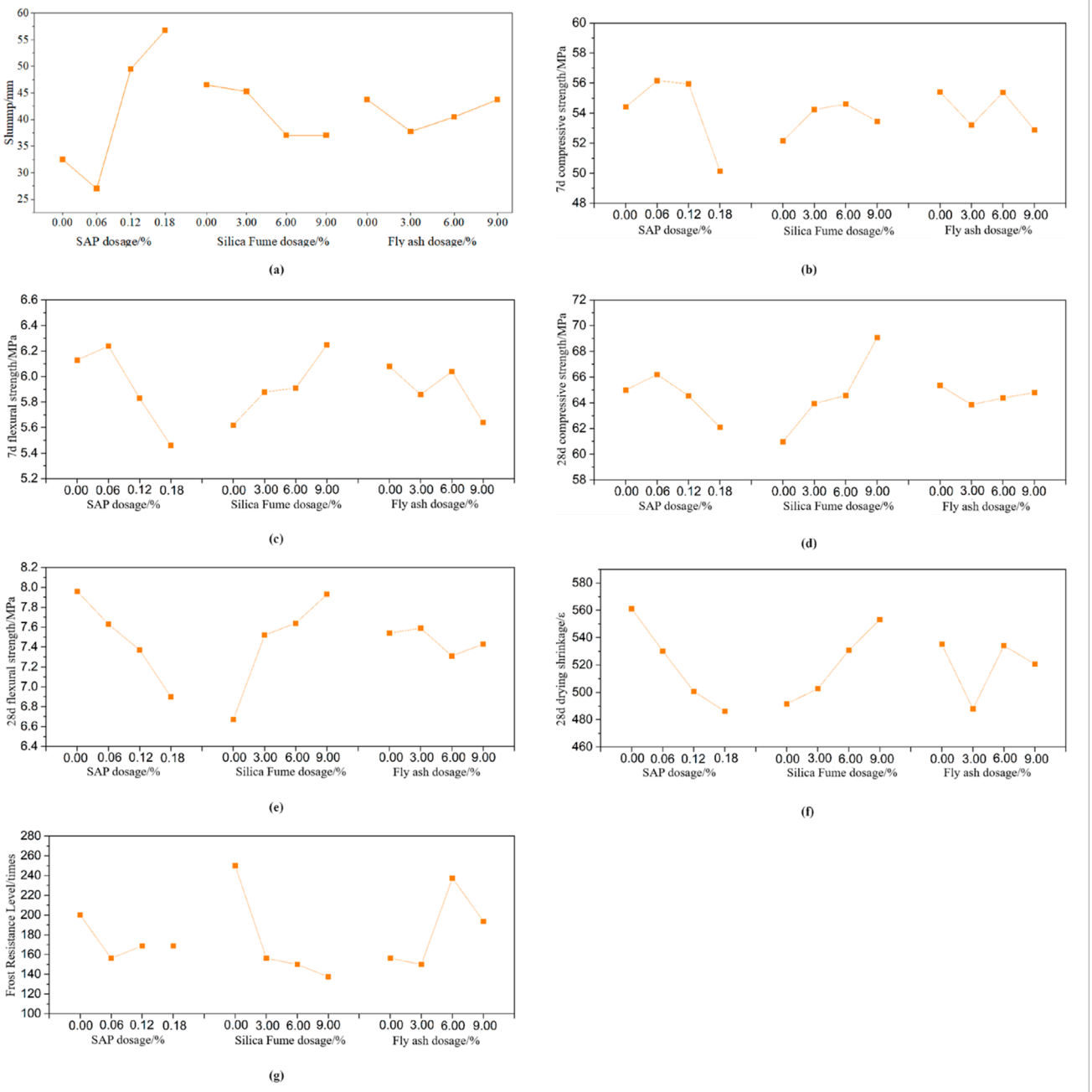

FIGURE 9
Influence of different factor levels on the performance of concrete. **(A)** Effect of different factor levels on the slump of concrete. **(B)** Influence of different factor levels on the 7-day compressive strength of concrete. **(C)** Influence of different factor levels on the 7-day flexural strength of concrete. **(D)** Influence of different factor levels on the 28-day compressive strength of concrete. **(E)** Influence of different factor levels on the 28-day flexural strength of concrete. **(F)** Influence of different factor levels on the 28-day drying shrinkage rate of concrete. **(G)** Influence of different factor levels on the freeze-thaw resistance grade of concrete.

of 13.30% in compressive strength. The effect of fly ash content on compressive strength was not significant.

As shown in Figure 9E, the 28-day flexural strength of concrete decreases with the increase in SAP content and increases with the increase in silica fume content, while the fly ash content has little effect on the 28-day flexural strength of concrete. When the SAP content is 0.00%, the 28-day flexural strength of the concrete is 7.96 MPa, and when the SAP content is 0.18%, the flexural strength decreases to 6.90 MPa, a reduction of 13.32%. When the silica fume content increases from 0.00% to 9.00%, the 28-day flexural strength increases by 18.89%. Therefore, it can be concluded that silica fume and SAP are two significant factors influencing the 28-day flexural strength of high-performance concrete for pavement.

As shown in Figure 9F, the 28-day drying shrinkage rate of high-performance crushed sand concrete decreases with the increase of SAP content and increases with the increase of micro-silica content.

10.3389/fmats.2025.1562267

TABLE 7 Optimal factor level combinations for various properties of concrete based on orthogonal testing.

Evaluation indicators	Optimal factor levels for each factor		
	A: SAP dosage %	B: silica fume dosage %	C: fly ash dosage %
Slump	A4	B2	C4
7d Compressive Strength	A2	B2	C1
7d Flexural Strength	A2	B1	C1
28d Compressive Strength	A2	B1	C1
28d Flexural Strength	A3	B1	C2
28d Dry Shrinkage Rate	A4	B4	C2
Freeze-Thaw Durability	A3	B4	C4

TABLE 8 Optimal factor levels for concrete based on main evaluation indicators.

Evaluation indicators	Optimal factor levels for each factor		
	A: SAP dosage %	B: silica fume dosage %	C: fly ash dosage %
28d Flexural Strength	A3	B1	C2
28d Dry Shrinkage	A4	B4	C2
Freeze Resistance Grade	A3	B4	C4

TABLE 9 Test results of L4 and L16 evaluation indexes under orthogonal test.

Test number	Combination scheme	Slump (mm)	Compressive strength (MPa)		Flexural strength (MPa)		28d dry shrinkage (10^{-6})	Freeze resistance Grade (times)
			7d	28d	7d	28d		
L4	$A_1B_4C_4$	45	53.07	60.17	5.63	6.35	479.6	300
L16	$A_4B_4C_3$	62	46.96	56.94	4.93	5.95	483.3	300

TABLE 10 Quantitative analysis of SAP.

Performance indicator	Per 0.01% SAP	Trade-off ratio
Slump	+1.389 mm	Increase in slump
7-day Compressive Strength	−0.233 MPa	For each 1 MPa loss in compressive strength ↔ shrinkage rate reduces by 18.8×10^{-6}
7-day Flexural Strength	−0.039 MPa	For each 1 MPa loss in flexural strength ↔ shrinkage rate reduces by 112.5×10^{-6}
28-day Compressive Strength	−0.167 MPa	For each 1 MPa loss in compressive strength ↔ shrinkage rate reduces by 26.3×10^{-6}
28-day Flexural Strength	−0.058 MPa	For each 1 MPa loss in flexural strength ↔ shrinkage rate reduces by 75.7×10^{-6}
Drying Shrinkage Rate	-4.389×10^{-6}	Reduction in drying shrinkage rate

TABLE 11 Mix ratio of high-performance machine-made sand concrete.

W/C	Constituent material/kg/m^3						
	Water	Cement	Fly ash	SAP	Sand	Crushed stone	Water reducing agent
0.37	155	357	63	0.18%	786	1179	1.2%

Specifically, the drying shrinkage rate of concrete is inversely proportional to the SAP content and directly proportional to the micro-silica content. When the SAP content is 0.18%, the 28-day shrinkage rate is 13.37% lower than when the SAP content is 0.00%. When the micro-silica content is 0.18%, the 28-day shrinkage rate increases by 12.53% compared to the 0.00% content. The 28-day drying shrinkage rate of concrete first decreases, then increases, and then decreases again as the fly ash content increases, showing an overall decreasing trend. This is because the fly ash content range is relatively small, and the substitution of cementitious materials is limited, leading to insignificant effects on the concrete performance. Therefore, SAP content can reduce the drying shrinkage rate of concrete, and within a certain range, the higher the SAP content, the lower the drying shrinkage rate of concrete. The inclusion of micro-silica increases the shrinkage rate of concrete, so its addition in arid regions may affect the shrinkage performance of concrete, leading to adverse effects.

As shown in Figure 9G, the freeze-thaw resistance grade of concrete initially decreases and then increases with the increase in SAP content. It decreases with the increase in silica fume content and increases and then decreases with the increase in fly ash content. Among these, the increase in silica fume content leads to the most significant decrease in the freeze-thaw resistance grade of concrete, with a reduction of 45%. The freeze-thaw resistance grade at 9.0% fly ash content is 24% higher than that at 0.00% content. Therefore, the incorporation of silica fume negatively affects the freeze-thaw resistance of concrete, while the inclusion of fly ash improves its freeze-thaw resistance.

3.8 Optimization of concrete mix design

The pavement concrete made from manufactured sand must withstand direct loads from traffic and other external forces, while also resisting the corrosion effects of the surrounding specific climatic conditions. Therefore, pavement concrete not only needs to meet basic workability requirements but must also possess high bending and tensile strength, along with satisfactory freeze-thaw durability and low shrinkage performance.

In light of this, the optimal factor levels for SAP, silica fume, and fly ash were analyzed based on their significant effects on 7-day compressive strength, 7-day flexural strength, 28-day compressive strength, 28-day flexural strength, 28-day drying shrinkage, and freeze-thaw resistance, with the results summarized in Table 7.

From Table 7, it can be seen that the SAP level with the most significant influence on all evaluation indicators is A2, the silica fume level is B1, and the fly ash level is C1. Therefore, the optimal solution based on the relationship between evaluation indicators and the corresponding optimal factor levels is A2B1C1. However, this solution does not meet the main requirements for the design of high-performance pavement concrete. Hence, the A2B1C1 solution is not considered.

On this basis, the 28d flexural strength, 28d dry shrinkage rate, and freeze-thaw durability are selected as the main evaluation indicators. The first two most significant factors affecting the performance of the pavement concrete are considered, along with the excellent freeze-thaw durability performance combinations in L4 and L16 of the orthogonal experiment. A comprehensive decision is then made to determine the mix proportion for pavement high-performance concrete under characteristic climate conditions. The optimal factor levels for the main evaluation indicators of pavement high-performance concrete are shown in Table 8, and the test results of each evaluation indicator for L4 and L16 in the orthogonal experiment are shown in Table 9, and the quantitative analysis of SAP is shown in Table 10.

From Table 8, it can be seen that the factors that have the greatest impact on the 28d flexural strength, 28d dry shrinkage, and freeze resistance grade of the pavement manufactured sand concrete are SAP and silica fume. The most significant levels of these influencing factors on the primary evaluation indicators are A3 and B4. Based on Table 9, it is found that the optimal content of silica fume is consistent with L4 and L16, while the optimal content of SAP varies. When the SAP content is 0.18%, it has the best effect on reducing the 28d dry shrinkage, but it causes a relative decrease in the flexural strength of the concrete. However, referring to the combination scheme and test results of L16, it can be seen that when the SAP content is 0.18%, the 28d flexural strength reaches 5.95 MPa, with a higher slump value and a freeze resistance grade of 300 cycles. The fly ash content is 9.0%, all of which meet the design requirements. Secondly, Table 10 demonstrates the trade-off between mechanical strength and durability. The optimized mix ratio results in a significant reduction in shrinkage and an improvement in freeze-thaw resistance, while only a slight sacrifice is made in compressive and flexural strengths. Additionally, extending fly ash content to 15% (exceeding orthogonal test levels) is proposed based on Cao et al. (2007) findings that 15%–20% fly ash optimally balances late-strength development (via continued pozzolanic reactions) and shrinkage resistance in pavement concrete. Considering all factors, the optimal combination of levels for the performance of the high-performance pavement manufactured sand concrete is A4B4C, the final decision is that the SAP content is 0.18%, the silica powder content is 0.00%, and the fly ash content is 15%.

The mix design for high-performance manufactured sand concrete is shown in Table 11.

4 Conclusion

This study employs an orthogonal experimental method to investigate the composition materials and optimization design of high-performance manufactured sand concrete for pavements. The study focuses on the durability and shrinkage properties of the concrete, aiming to determine the mix ratio under characteristic climatic conditions. Based on this, microscopic testing methods and mechanism analysis are applied to further reveal the intrinsic relationship between the microstructure and macroscopic properties. The conclusions are as follows:

(1) The mechanical properties of high-performance manufactured sand concrete decrease with the increase in SAP content, while they improve with the increase in the content of silica fume and fly ash.
(2) As the SAP content increases, the shrinkage rate of high-performance manufactured sand concrete for pavements gradually decreases, indicating that the incorporation of SAP in the concrete can reduce its shrinkage rate and enhance the shrinkage resistance of the pavement concrete.
(3) The frost resistance degradation pattern of high-performance manufactured sand concrete is as follows: when the number of freeze-thaw cycles does not exceed 50, the degradation of frost resistance is slow. Between 50 and 150 freeze-thaw cycles, the degradation rate of frost resistance increases sharply. After 150 freeze-thaw cycles, the degradation rate gradually slows down until freeze-thaw failure occurs.
(4) In terms of the microstructure of the concrete, as the number of freeze-thaw cycles increases, the hydration products of the concrete gradually decrease, and the microstructure density of the concrete gradually becomes more porous. After 150 freeze-thaw cycles, the concrete with 0.18% SAP content exhibits a relatively higher microstructural density.
(5) The optimal performance of high-performance manufactured sand concrete for pavements is achieved when the water-to-cement ratio is 0.37, the sand ratio is 42%, the SAP content is 0.18%, the silica fume content is 0.00%, the fly ash content is 15%, and the water-reducing agent content is 1.2%.
(6) Practitioners in seasonal frozen regions should prioritize the optimized mix (0.18% SAP, 15% fly ash, 0% silica fume) for pavements requiring high durability. Field trials are recommended to validate long-term performance under traffic loads. Future research should explore SAP's pore-structure dynamics via MIP and assess scalability in diverse climatic conditions.

5 Prospect

This study focuses on the composition and performance of high-performance manufactured sand cement concrete for pavements under the specific climatic conditions of Lanzhou, China. The research primarily investigates the mechanical properties, frost resistance, durability, and drying shrinkage performance of this type of concrete. However, due to limitations in experimental conditions, insufficient research time, and other factors, certain shortcomings remain. Based on reflections during the research process, the following suggestions are proposed for future studies:

(1) This study examined the frost resistance of high-performance manufactured sand concrete with varying SAP dosages. However, due to certain constraints, techniques such as MIP were not utilized to investigate the influence of SAP on concrete freeze-thaw behavior from the perspective of pore structure changes. It is recommended that future research focus on the effects of SAP on the pore structure of concrete.
(2) The experiments in this study were primarily conducted in laboratory settings, and no field test sections were laid for long-term observation. Therefore, it is suggested to conduct test pavement sections in other cold and arid regions to observe the coupled effects of cold and arid conditions on the performance of high-performance manufactured sand concrete for pavements over extended periods.
(3) Field validation is critical for translating laboratory findings. Preliminary insights suggest that the optimized mix's high workability (slump = 62 mm) and frost resistance (300 cycles) align with practical requirements, but onsite adjustments may be needed for temperature fluctuations and construction practices.

Data availability statement

The original contributions presented in the study are included in the article/supplementary material, further inquiries can be directed to the corresponding author.

Author contributions

CH: Conceptualization, Data curation, Formal Analysis, Funding acquisition, Supervision, Validation, Writing–original draft. JZ: Data curation, Methodology, Project administration, Visualization, Writing–review and editing. HR: Data curation, Investigation, Project administration, Software, Visualization, Writing–review and editing. XY: Conceptualization, Funding acquisition, Methodology, Project administration, Resources, Software, Visualization, Writing–original draft, Writing–review and editing.

Funding

The author(s) declare that no financial support was received for the research, authorship, and/or publication of this article.

Conflict of interest

The authors declare that the research was conducted in the absence of any commercial or financial relationships that could be construed as a potential conflict of interest.

Generative AI statement

The author(s) declare that no Generative AI was used in the creation of this manuscript.

Publisher's note

References

Bertelsen, I. M. G., Ottosen, L. M., and Fischer, G. (2020). Influence of fibre characteristics on plastic shrinkage cracking in cement-based materials: a review. *Constr. Build. Mater.* 230, 116769. doi:10.1016/j.conbuildmat.2019.116769

Cai, J., Li, B., Zhou, M., and Hu, X. (2006). Effects of crusher dust on properties of low/medium strength concrete with manufactured sand. *J. Wuhan Univ. Technol.*, 27–30. doi:10.1016/S1872-1508(06)60035-1

Cao, C., Zhang, W., and Wang, Y. (2007). *Experimental study on the application performance of high admixture fly ash concrete pavement*. J. Tongji Univ. 35, 6. doi:10.1016/S1672-6529(07)60007-9

Chinese Standards (2006). Technical specification for application of high-performance concrete.

Chinese Standards (2010). Standard test method for long term performance and durability of ordinary concrete.

Chinese Standards (2017). Standard for test method of performance on ordinary fresh concrete.

Chinese Standards (2019a). Standard for test methods of concrete physical and mechanical properties.

Chinese Standards (2019b). Technical Guidelines for construction of Highway cement concrete pavements.

Chinese Standards (2021). Testing methods of cement and concrete for Highway engineering.

Chinese Standards (2022). Construction sand.

Chitthawornmanee, S., Kaur, H., Tran, T. N.Ho, Chindasiriphan, P., Jongvivatsakul, P., and Tangchirapat, W. (2025). Influences of superabsorbent polymer (SAP) on the compressive strength and crack-healing ability of self-compacting concrete containing high-volume ground bottom ash. *Case Stud. Constr. Mater.* 22, e04196. doi:10.1016/j.cscm.2024.e04196

Craeye, B., Geirnaert, M., and Schutter, G.De (2011). Super absorbing polymers as an internal curing agent for mitigation of early-age cracking of high-performance concrete bridge decks. *Constr. Build. Mater.* 25, 1–13. doi:10.1016/j.conbuildmat.2010.06.063

Hansen, J. P. F. (2001). Water-entrained cement-based materials: I. Principles and theoretical background. *Cem. Concr. Res.* doi:10.1016/S0008-8846(01)00463-X

He, R., and Lu, Na (2024). Hydration, fresh, mechanical, and freeze-thaw properties of cement mortar incorporated with polymeric microspheres. *Adv. Compos. Hybrid Mater.* 7, 92. doi:10.1007/s42114-024-00899-2

Hoque, Md A., Shrestha, A., Sapkota, S. C., Ahmed, A., and Paudel, S. (2025). Prediction of autogenous shrinkage in ultra-high-performance concrete (UHPC) using hybridized machine learning. *Asian J. Civ. Eng.* 26, 649–665. doi:10.1007/s42107-024-01212-8

Ju, Y., Zhang, L., and Wang, D. (2013). Durability study of activated powder concrete for road use in monsoon freezing zone. *Concrete*, 60–63. doi:10.3969/j.issn.1002-3550.2013.08.016

Lao, J., Huang, Z., Guo, Y., Chen, L., Shen, A., and Yang, J. (2021). *Study on shrinkage properties and mechanical properties of pavement concrete raised in SAP silicate bulletin*. Bulletin of The Chinese Ceramic Society, 40, 676–682. doi:10.16552/j.cnki.issn1001-1625.2021.02.039

Li, L., Chai, H., Hu, Y., He, R., and Wang, Z. (2024). Feasibility study on superabsorbent polymer (SAP) as internal curing agent for cement-based grouting material. *Constr. Build. Mater.* 411, 134286. doi:10.1016/j.conbuildmat.2023.134286

Li, Z. (2009). *Study on the anti-salt and frost spalling performance of road concrete in cold areas*. J. Harbin Univ. doi:10.7666/d.D257308

Liu, J., Farzadnia, N., Shi, C., and Ma, X. (2019). Effects of superabsorbent polymer on shrinkage properties of ultra-high strength concrete under drying condition. *Constr. Build. Mater.* 215, 799–811. doi:10.1016/j.conbuildmat.2019.04.237

Liu, S., Liu, X., and Zhang, J. (2013). Design of active powder concrete proportion based on orthogonal test. *Highway*. pp. 158–160. doi:10.3969/j.issn.0451-0712.2013.02.035

Mechtcherine, V., Secrieru, E., and Schröfl, C. (2015). Effect of superabsorbent polymers (SAPs) on rheological properties of fresh cement-based mortars — development of yield stress and plastic viscosity over time. *Cem. Concr. Res.* 67, 52–65. doi:10.1016/j.cemconres.2014.07.003

Snoeck, D., Goethals, W., Hovind, J., Trtik, P., Belie, N.De, Van den Heede, P., et al. (2021a). Internal curing of cement pastes by means of superabsorbent polymers visualized by neutron tomography. *Cem. Concr. Res.* 147, 106528. doi:10.1016/j.cemconres.2021.106528

Snoeck, D., Goethals, W., Hovind, J., Trtik, P., Van Mullem, T., Van Den Heede, P., et al. (2021b). Internal curing of cement pastes by means of superabsorbent polymers visualized by neutron tomography. *Cem. Concr. Res.* 147, 106528. doi:10.1016/j.cemconres.2021.106528

Snoeck, D., Pel, L., and De Belie, N. (2017). The water kinetics of superabsorbent polymers during cement hydration and internal curing visualized and studied by NMR. *Sci. Rep.* 7, 9514. doi:10.1038/s41598-017-10306-0

Wang, S., Ma, G., Zhu, Z., Liu, X., Wu, Y., and Guo, X. (2007). Design of high performance pavement concrete proportions. *Highw. Transp. Technol.*, 25–28. doi:10.3969/j.issn.1002-0268.2007.04.006

Xu, J., Li, F., Wang, B., Luo, X., Chen, G., and Wang, H. (2004). *Research on antifreeze properties of poor concrete for road subgrade*. J. Harbin Univ. Technol, 134–136. doi:10.3321/j.issn:0367-6234.2004.01.037

Yan, X., Yang, H., and Shi, Y. (2011). Study of limestone powder mixing in sand on concrete properties. *Concrete*, 67–69. doi:10.3969/j.issn.1002-3550.2011.11.020

Yu, B., and Chen, Y. (2021). Experiment on control measures of shrinkage and cracking of high strength manufactured sand concrete containing a large amount of high absorbency stone powder. *Acta Mater. Compos. Sin.* 38, Article 2737. doi:10.13801/j.cnki.fhclxb.20210430.001

Yuan, C. Y., Shen, A. Q., Han, J. G., and Zhao, L. Y. (2007). Durability of high performance pavement concrete with fine slag. *J. China Journal of Highway and Transport* (05), 24–29. doi:10.19721/j.cnki.1001-7372.2007.05.005

Zhang, M., Liu, T., Yang, H., Xu, J., and Wang, Y. (2024). Crack resistance, permeability, and microstructural analysis of recycled aggregate concrete with SAP. *Constr. Build. Mater.* 430, 136479. doi:10.1016/j.conbuildmat.2024.136479

Zhang, Q., Sun, H., Liu, W., Zhou, Z., Yuan, L., Ren, Z., et al. (2021). Effect of rGO on the mechanical strength, hydration and micromorphology of cement incorporated silica fume. *Constr. Build. Mater.* 300, 124325. doi:10.1016/j.conbuildmat.2021.124325

Zhou, M., Wang, J., Zhu, L., and He, T. (2008). Effects of manufactured-sand on dry shrinkage and creep of high-strength concrete. *J. Wuhan Univ. Technology-Mater* 23, 249–253. doi:10.1007/s11595-006-2249-5